2020-09

Weld solidification cracking in a 304L stainless steel water tank

James, MN

10.1016/j.engfailanal.2020.104614
Engineering Failure Analysis
Elsevier BV

Weld Solidification Cracking in a 304L Stainless Steel Water Tank

M N James [1,2], L Matthews [2] and D G Hattingh [2]

[1] School of Engineering, Computing & Mathematics, University of Plymouth, Plymouth, England
[2] eNtsa, Nelson Mandela University, Port Elizabeth, South Africa

Abstract: Type 304L stainless steel alloy is known to be highly resistant to solidification cracking. In the present case the particular design of the welded seams in a simple 200 litre water tank, along with the likely manner in which the closing welds were made, has led to an interesting example of interdendritic hot cracking in 304L GTA welded using a 309L filler metal. The paper presents a short introduction to hot cracking in austenitic stainless steels and uses the fractographic evidence to demonstrate that this form of cracking has occurred. The cracking has occurred primarily from excessive residual restraint stresses arising from weld -fit-up and welding practice, combined with the particular sequence of welds made in finally closing the tank.

Keywords: Solidification cracking; 304L stainless steel; weld process; weld restraint

Introduction

Hot cracking in austenitic stainless steels has been widely investigated for many years, with significant progress being made both in classifying it and in understanding the causes of such cracking, e.g. [1-6]. It is therefore the case that welding of stainless steel alloys such as 304L using either autogenous GTAW, or GTAW with a 308 or 309 alloy filler metal, is generally straightforward with useful information on joint design and welding conditions being widely available. The hot cracking phenomenon is, however, rather subtle and can be significantly influenced by heat flow during welding, i.e. weld process conditions, and by aspects of joint design, fit-up, restraint and weld sequencing.

Cases of hot cracking in 304L stainless steel welded with a 309L filler metal are relatively scarce, and it is therefore instructive to examine those which do occur, in the light of the published information regarding hot cracking and its avoidance, and to analyse the root causes of the failure. Thus this paper presents an example of solidification cracking that occurred in a seam weld made in 2 mm thick 304L stainless steel plate used to fabricate a 200 litre water tank. It starts by summarising a selection of the published work dealing with hot cracking of austenitic stainless in order to provide an overview of some of the subtleties associated with the occurrence of hot cracking and set the observed failure in context. The case study is interesting because it highlights the importance of some of these subtleties that can contribute to hot cracking and which may be overlooked in weld design and fabrication. In addition, this failure demonstrates an example where solidification cracking has occurred both as gross interdendritic cracking during welding, which then extended by fatigue, and as microfissuring in the interdendritic regions which only opened up under subsequent external loading [2].

Solidification Cracking in Austenitic Stainless Steels

Hot cracking can occur above the liquation temperature, where it is referred to as supersolidus cracking and in the solid state, which is called subsolidus cracking [2]. Supersolidus cracking occurs either as solidification cracking in the presence of a liquid phase in the fusion zone, or as liquation cracking in the heat-affected zone (HAZ). Solidification cracking in the weld metal is considered to be the most deleterious and is more widely observed [2].

In general, as noted by Yu et al [4], austenitic stainless steels are less susceptible to solidification cracking when the primary solidification phase from the molten weld metal is δ-ferrite (body-centred cubic structure) rather than the austenite (γ) face-centred cubic structure that represents the parent plate at ambient temperature. Shankar et al [2] in their very useful overview of solidification cracking in austenitic stainless steels considered the forms that solidification cracking can take. They note that it can occur as either gross cracking at the interdendritic junctions, where it is detectable by visual or dye penetrant inspection, or as microfissuring in the interdendritic regions which only becomes apparent when the welded joint is subject to strain.

Factors such as alloy composition and heat input during welding are well known to influence the weld metal composition in austenitic alloys and Shankar et al [2] give a useful discussion of the effects of δ-ferrite and solidification mode on cracking behaviour. They observe that although early work identified the percentage of weld metal δ-ferrite as conferring resistance to cracking, later work found that the mode of solidification was the controlling factor. The primary solidification mode is a function of alloy composition and the ferrite/ferrite-austenite (F/FA) mode is beneficial in reducing cracking. Subsequently, various authors used hot cracking tests to rank commercial alloy compositions in terms of susceptibility to solidification cracking.

Kujanpää, David and White [1] plotted the Schaeffler value for the ratio of Cr and Ni equivalents against the sum of the phosphorous and sulphur. They found that crack susceptible compositions were bounded by a curve with a lower limit of 0.01-0.15 wt.% and Cr_{eq}/Ni_{eq} values < 1.5. This diagram was modified by Lundin et al [7] using varestraint test data from 3 mm thick specimens, with the Cr_{eq}/Ni_{eq} ratio developed by Hammar and Svensson [8] (i.e. Cr_{eq} = Cr + 1.37Mo and Ni_{eq} = Ni + 0.31Mn + 22C + 14.2N). Lundin classified the alloy compositions via total crack length in the varestraint test at 4% strain. In the region of Cr_{eq}/Ni_{eq} ratios of 1.5-1.6, cracking was found to be sensitive to P+S levels. Varol, Baeslack and Lippold [3], also studied 304L and a duplex stainless steel using the varestraint test with imposed strains of 3.1% and 5%. In their varestraint test apparatus, solidification cracking in a fully austenitic type 304L weld were associated with relatively straight austenite grain boundaries. In contrast, cracks in type 304 with 8% ferrite weld metal were very short and not as clearly associated with fusion zone grain boundaries.

Weld process conditions also have a strong effect on hot cracking behaviour, with both heat input [2] and solidification rate [9] playing a role in crack susceptibility. The work by Hochanadel et al [9] is particularly relevant in terms of weld solidification cracking in type 304 stainless steel, as they made annulus welds between types 304 and 304L coaxial tubes using pulsed laser beam welding and pulsed gas tungsten arc welding (GTAW). In their case, both alloy compositions should have been crack-free according to the WRC-1992 constitution diagram [10], that has replaced the Schaeffler [11] and DeLong [12] diagrams in prediction of weld microstructure. However, the composition range along the tie line between the two alloys, i.e. the range of weld metal compositions, passed through the crack-susceptible range. They concluded that their work demonstrated that crack susceptibility was influenced by heat-to-heat alloy variations in nominally weldable alloys and by variations in weld heat input and solidification rate. Work by Bermejo et al [13] on a wide range of austenitic grades, including commercial 304 alloy, supported the conclusion that high cooling rates and rapid solidification promoted austenitic solidification and extended the solidification cracking risk to a wider range of alloy compositions, assessed in terms of the ratio of chromium equivalent to nickel equivalent value (Cr_{eq}/Ni_{eq}) that is used in the WRC-1992 diagram.

The brief discussion given above of solidification cracking in austenitic stainless steel, highlights the point that care has to be taken to avoid the problem of hot cracking even when the chosen alloy is resistant to solidification cracking. This point is illustrated in the failure discussed in the present paper, where a seam weld in a type 304L stainless steel alloy water tank failed prematurely. The water tank had been installed on a vehicle which was then delivered by road to the customer over a distance of approximately 1,000 kilometres. At this point, part of the seam weld was found to be leaking. The customer inspected the failure by inserting a screwdriver into the failed seam, upon which the crack extended along the seam by a considerable distance. The failed tank was then provided for a failure investigation into the cause and mechanisms of the cracking, as a number of similar tanks were already in service.

This case study highlights several relevant issues in avoiding solidification cracking, including the importance of joint design and fit-up before welding, welding process conditions and joint restraint. As noted by Varol, Baeslack and Lippold [3] weld solidification cracking requires the simultaneous presence of a crack-susceptible microstructure and a threshold level of weld restraint, which is influenced by factors like joint fit-up and weld length. It also demonstrates an example of solidification cracking occurring both as gross interdendritic cracking and as microfissuring in the interdendritic regions which only became apparent when the welded joint was strained during insertion of the screwdriver tip into the crack.

The Welded Tank

The rectangular 200 litre water tank is shown in Figure 1 and is formed by welding together two pieces of type 304L stainless steel, each bent into a 'U' shape (Figure 1a), to complete the rectangular shaped tank (Figure 1b). Horizontal dimensions in Figure 1 are 640 mm by 662 mm with a vertical height of 504 mm. Chemical composition of the 304L alloy was measured using spectroscopy and the data is given in Table 1. The alloy conforms to the specification for commercial 304L plate and it should be highly resistant to solidification cracking.

Table 1 Chemical composition of the 304L alloy

	Cr	Ni	C	Mn	P	S	Si	Cu	Mo	N	Fe
Tank	17.65	8.13	0.033	1.31	0.022	0.008	0.50	0.162	0.18	0.022	Bal.
Spec. 304L	18.0-20.0	8.0-12.0	0.03 max	2.00 max	0.045 max	0.030 max	0.75 max	-	-	0.10 max	Bal.
Spec. 309L	23.0-25.0	12.0-14.0	0.03 max	1.00-2.50	0.030 max	0.030 max	0.30-0.65	0.75 max	0.75 max		

The welded seams on one side of the tank are marked with the letters 'A1' to ‘A3’ with the welding sequence apparently following A1 → A2 → A3. Welding on the opposite side presumably followed an equivalent sequence and closure of the tank was accomplished via welds B1 and B2. The crack origin was approximately in the centre of one of the 640 mm sides, as shown with the red dotted shape in Figure 1b and the arrow in Figure 1c. The hole shown in the top surface is where the filling valve for the tank is located and there is an internal baffle plate that extends to the half-height position. This baffle plate was tack welded on the

vertical sides and bottom of the tank, but free on the top surface. The baffle plate welding showed that tank closure had been achieved by making the welds A1, A2 and A3, probably continuously in that order. Hence a considerable restraint on the seam weld A3 would have arisen during solidification from the residual stresses induced during cooling by this welding sequence.

Welding was performed using a GTAW process with a type 309L filler metal (chemical composition given in Table 1). However, the tank manufacture had been subcontracted the water tank designer, and it proved to be impossible to obtain details of the welding process used. What is clear, however, is that the weld was poorly detailed in the drawings and that the process used was inappropriate in at least some of the details. The weld crown was subsequently ground to provide a smooth transition before painting the tank (see Figure 2).

The finished tank was then mounted on a vehicle, filled with water and driven around 1,000 km to the customer. On arrival at its destination, water was noticed leaking from one of seam welds. In examining the leak, the customer was stated to have inserted a screwdriver into the leaking seam, and this caused the flaw to extend a considerable distance reportedly with an audible crack. The tank was subsequently returned to the manufacturer and sent for an investigation into the cause and mechanism of failure.

Fractography

A piece of the weld seam, some 200 mm in length, that contained the complete fracture was sectioned from the failed joint (shown in Figure 1c). An adjacent piece was also cut out to allow measurement of the reduction in plate cross-section arising from the corner grinding. Figure 2 shows that this cosmetic attention to detail reduced the metal thickness at the critical weld root position, which coincides with the presence of a small crack, from 2.04 mm to 1.34 mm, equivalent to a reduction of 34%. The sharp weld root and its associated defect is shown at higher magnification in Figure 3. The defect has a total length of around 100 μm. It started from a partial penetration defect (A), and comprises a sharp weld toe intrusion (B) and a final section of cracking that occurred during welding (C). The blue and straw yellow temper colours seen in Figure 4 prove that the initial crack extension occurred during welding and that it is therefore due to an embrittlement problem. Figure 3 indicates that the cracking occurring during welding was assisted by the presence of a sharp weld toe intrusion resulting from undercut at a partial penetration weld.

Part of the fracture surface containing the original through-thickness crack (indicated by screwdriver damage on the fracture surface – Figure 5) was sectioned from the larger specimen, cleaned and mounted for fractographic examination with stereo binoculars and with a scanning electron microscope. Low magnification inspection using stereo binoculars showed that a number of beachmarks were present both in the region of the initial water leak (Figure 5) and more generally along the fracture (Figure 6). The considerable number of beachmarks through the thickness indicates that their formation cannot be due only to a change in fracture mechanism from the pre-existing solidification crack to subsequent fatigue crack growth and/or fast fracture.

Figure 7 shows an scanning electron microscopy (SEM) fractograph of the complete fracture surface for comparison with the light fractograph in Figure 6 and to approximately locate the position of subsequent images of the fracture mechanisms. An arrow marks the same inclusion in both Figures 6 and 7. Figure 8 depicts the initial part of the fracture surface (seen in section in Figure 3) which contains the partial penetration defect, a sharp weld root intrusion

resulting from undercut (marked in the image) and the initial region of the solidification crack. The microvoids reflect the high temperature at which the solidification cracking occurred and their size is likely to be related to the dendritic interstices.

A fatigue mechanism is believed to have caused crack extension through the seam weld thickness during delivery of the water tank to the customer. The tank is never completely filled with water and will experience slosh during the delivery journey, while the very sharp weld toe intrusion crack would require only small applied stresses to grow. It is also possible that a resonance problem existed, where a natural frequency of the tank coincided with the frequency of road-induced vibration. In this respect Figure 9 shows the transition from the initial solidification defect to a fracture mechanism that is typical of slow fatigue crack growth in 300 series austenitic stainless steels, where occasional intergranular facets reflect an environmental component to crack growth e.g. [14].

Moving further from the root of the weld, Figure 10 indicates that the fracture surface mechanism changes to one that represents brittle interdendritic fracture, with the possible origin being loads arising from liquid slosh during heavy braking or accelerating, or from significant irregularities in the road surface, e.g. potholes. The beachmarks on the fracture surface (Figures 5 and 6) can therefore be ascribed to a sequence of changes from one interdendritic interface to another. This is proposed to be a result of microfissuring in the interdendritic regions opening up into a crack under strains induced during transportation of the tank [2]. This interdendritic mechanism is clearly seen in Figure 11 at higher magnification and was also the mechanism involved in the crack extension when the screwdriver was inserted into the original crack.

Discussion

Guidance on GTAW of common welded joints is widely available on the internet, e.g. [15] and the full-open or half-open corner joint that was used for the failed seam weld (illustrated in Figure 12), although simple, requires some attention in terms of fit-up. According to the guide in reference [15] open corner joints demand precise fixturing because of the shallow joint depth and the ease with which the edge of the material melts. Stainless steel open corner joints are particularly susceptible to warping and tack welds may be required at a spacing ~50-75 mm in thin material to maintain a consistent joint. There was no evidence of such tack welds being used in the present case.

The throat of the weld should be at least the thickness of the parent plate and a fast travel speed is required to avoid melt-through to the inside corner. However, a fast travel speed is likely to result in a lower heat input per millimetre and a faster cooling of the joint which can then trigger solidification cracking. The torch angle should bisect the angle formed by the two pieces of metal to be joined in order to apply equal heat to both sides of the joint. As can be seen in Figure 2, the heat input does not appear to be uniform in the two sides of the joint and this has led to the sharp lack-of-penetration defect, associated weld root undercut and the resultant solidification cracking from a combination of high joint restraint and fast cooling (Figure 4).

The crack extension from insertion of a screwdriver into the initial leaking fissure reflected the extensive interdendritic solidification microfissuring across the throat of the weld (Figures 10 and 11).

A change in welding practice should resolve this problem, although a redesign of the tank could also be undertaken utilising, for example, rolled plate with a single butt weld joint and a flanged approach to attaching top and bottom pieces. These could then be either bolted or employ an edge weld on the flanged corner.

Conclusions

A water tank fabricated from 304L alloy using a GTAW process with a 309L alloy filler metal should normally be expected to be highly resistant to solidification cracking. This particular tank has, nonetheless, experienced this form of cracking as a result of inadequate design specification, fabrication and welding practice. A relatively straightforward stainless steel manufacturing operation has been turned into an expensive repair and redesign issue, as a number of tanks were delivered and at least one other tank has so far demonstrated the same cracking problem.

Solidification cracking in a 304L stainless steel GTA welded with a 309L filler metal is unusual, but the reported cracking events, along with the fractographic evidence show that this form of cracking has occurred. Yu et a [4] have demonstrated that solidification cracking in austenitic stainless steel can be significantly affected by the liquid-δ-γ reaction during solidification, although it is not clear what has happened in the present case. The most likely explanation is that obstructed shrinkage during mushy zone solidification has led to cracking along interdendritic boundaries during the latter stage of solidification, where a small amount of liquid remains along grain boundaries that is sufficient to keep grains from bonding, but insufficient to completely fill the interdendritic spaces under the applied tension stress [4]. This obstructed shrinkage has arisen because of the way that the tank was designed and fabricated with a single long continuous weld run apparently being used to close the tank.

The case study is interesting in that it highlights the potential for hot cracking to occur in 304L if the weld design specification, fit-up, process conditions and welding practice are not sufficiently well-controlled.

References

1. Kujanpää, V.P., S.A. David, and C.L. White, *Formation of Hot Cracks in Austenitic Stainless Steel Welds—Solidification Cracking.* Welding Research Supplement, 1986. **08**(August): p. 203-s - 212-s.
2. Shankar, V., et al., *Solidification cracking in austenitic stainless steel welds.* Sadhānā, 2003. **28**(3 & 4): p. 359-382.
3. Varol, I., W.A. Baeslack III, and J.C. Lippold, *Characterization of Weld Solidification Cracking in a Duplex Stainless Steel.* Metallography, 1989. **23**(1): p. 1-19.
4. Yu, P., et al., *Microstructure Evolution and Solidification Cracking in Austenitic Stainless Steel Welds.* Welding Journal Supplement, (November 2018): p. s301-s314.
5. Yuan, J., M. Gao, and X. Zeng, *Study on microstructure and mechanical properties of 304 stainless steel joints byTIG, laser and laser-TIG hybrid welding.* Optica and Lasers in Engineering, 2010. **48**: p. 512-517.
6. Singh, S., K. Hurtig, and J. Andersson, *Investigation on effect of welding parameters on solidification cracking of austenitic stainless steel 314.* Procedia Manufacturing, 2018. **25**: p. 351-357.
7. Lundin, C., et al., *Weldability and hot ductility behavior of nuclear grade austenitic stainless steels.* Welding Research Council Bulletin, 2006: p. 1-266.

8. Hammar, O. and U. Svensson. *Influence of steel composition on segregation and microstructure during solidification of austenitic stainless steels*. in *Solidification and Casting of Metals*. 1979. Sheffield, England: The Metals Society.
9. Hochanadel, P., et al. *Weld Solidification Cracking in 304 to 304L Stainless Steel*. in *Hot Cracking Phenomena in Welds III*. 2011. Springer.
10. Kotecki, D.J. and T.A. Siewert, *WRC-1992 Constitution Diagram for Stainless Steel Weld Metals: A Modification of the WRC-1988 Diagram.* Welding Research Supplement, (May 1992): p. s171-s178.
11. Schaeffler, A.L., *Constitution diagram for stainless steel weld metal.* Mertal Progress, 1949. **56**(11): p. 680.
12. DeLong, W.T., *Ferrite in austenitic stainless steel weld metal.* Welding Journal Supplement. **53**(July 1974): p. s273-s286.
13. Bermejo, M.-A.V., et al., *Towards a Map of Solidification Cracking Risk in Laser Welding of Austenitic Stainless Steels.* Physics Procedia, 2015. **78**: p. 230-239.
14. Martelo, D.F., A. Mateo, and M.D. Chapetti, *Crack closure and fatigue crack growth near threshold of a metastable austenitic stainless steel.* International Journal of Fatigue, 2015. **77**: p. 64-77.
15. Miller. *GTA Welding Common Joint Designs* 2020; Available from: https://www.millerwelds.com/resources/article-library/gta-welding-common-joint-designs.

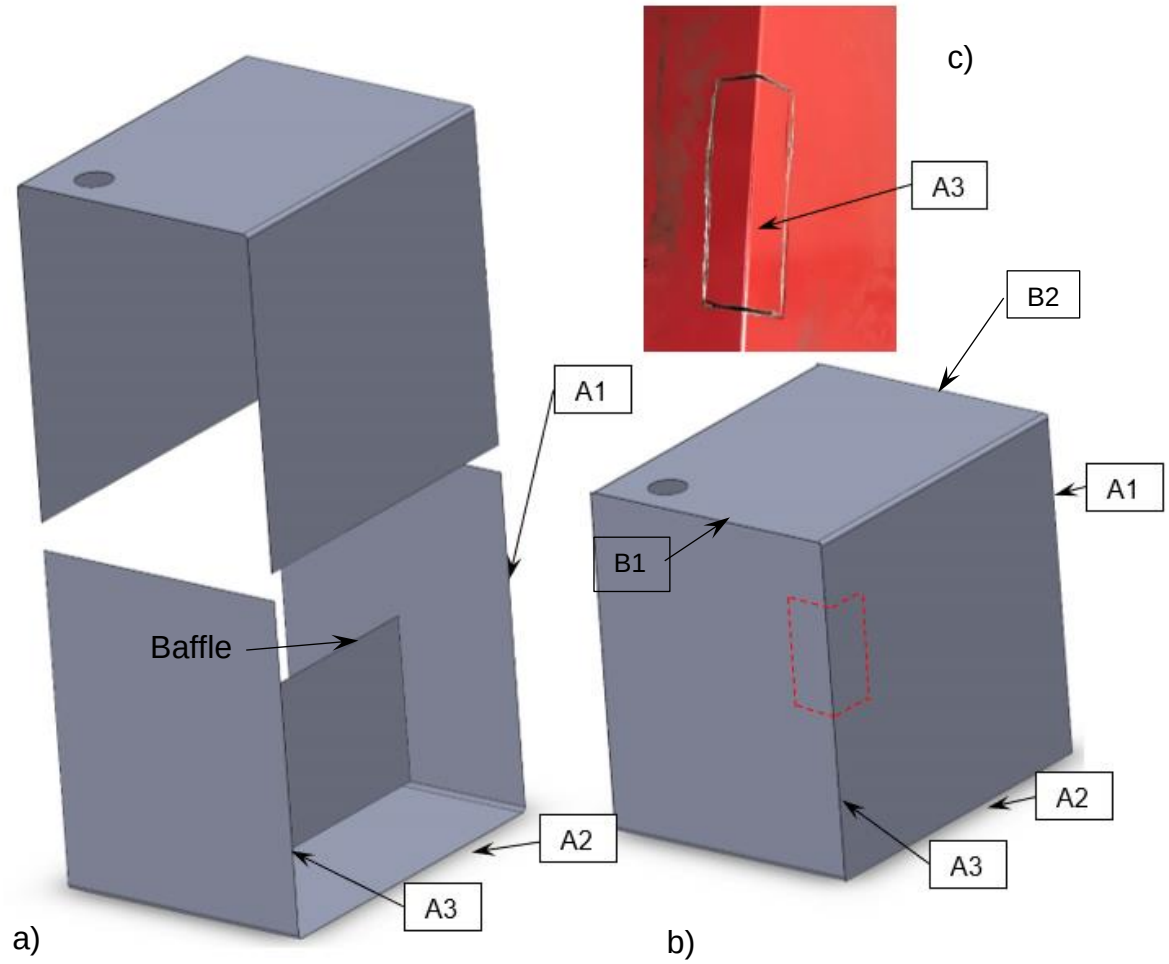

Figure 1 Illustrations of the water tank and its design; welding of the two sections occurred in the sequence of A1 → A2 → A3:
a) An exploded view of the two tank sections that were bent to form 'U'-shapes and were then welded together to make the tank. The position of an internal baffle is also shown.
b) The assembled water tank showing the position where seam cracking was found (red dotted rectangle on corner A3).
c) The actual sample that was sectioned from the tank for further analysis.

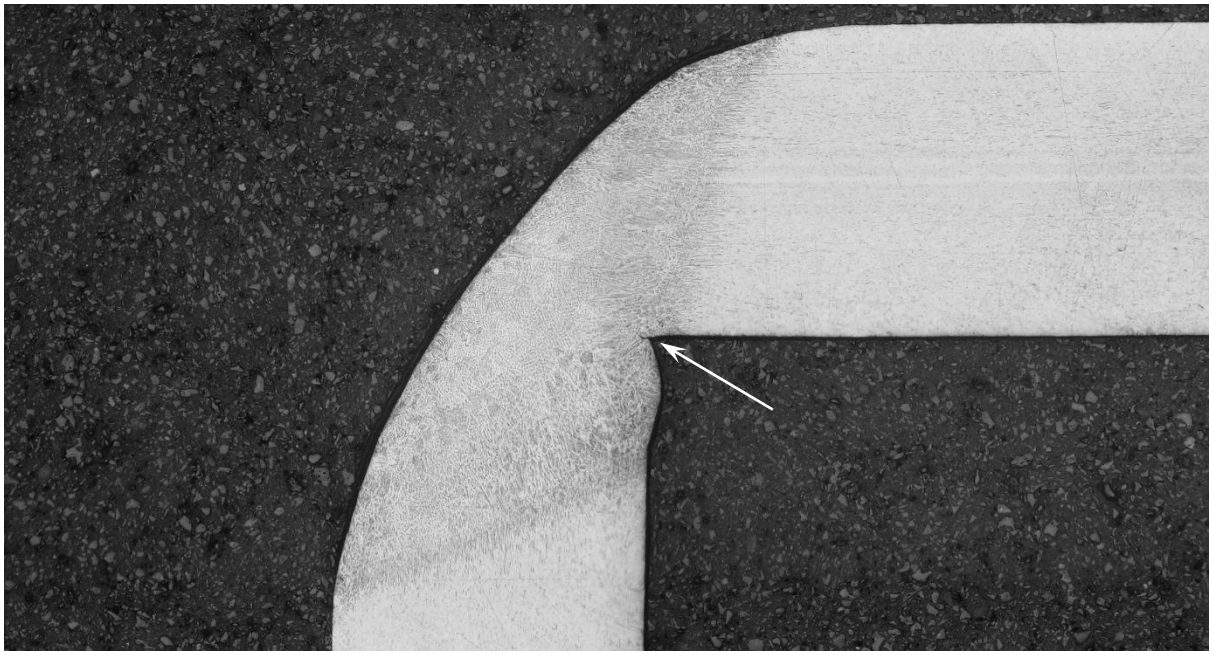

Figure 2 Macro-etched section of the seam weld that cracked, showing the reduction in thickness at the critical region where there is a small weld root crack (marked with the arrow).

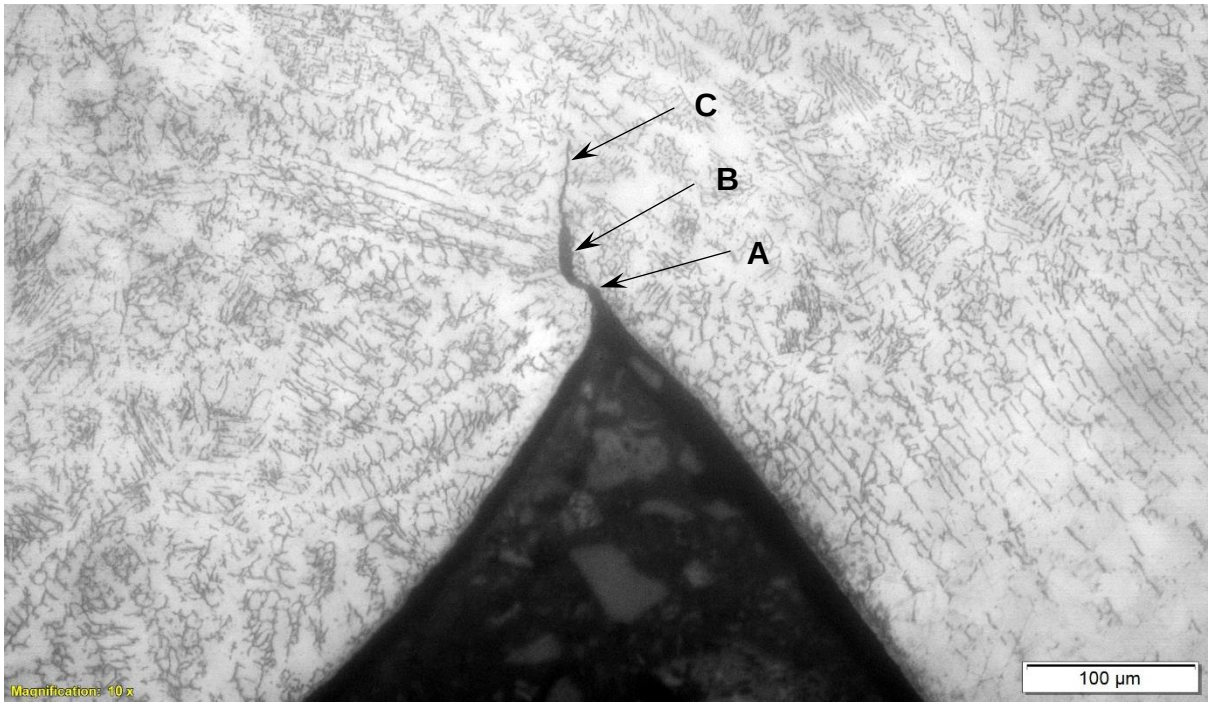

Figure 3 Higher magnification image of the weld root crack induced during welding. The crack has a total length of around 100 µm. It starts from a partial penetration defect (A), and comprises a sharp weld toe intrusion (B) and a final section of solidification cracking (C).

Figure 4 The fracture surface showing evidence of blue and straw temper colours, proving that the crack originated as a hot crack during solidification.

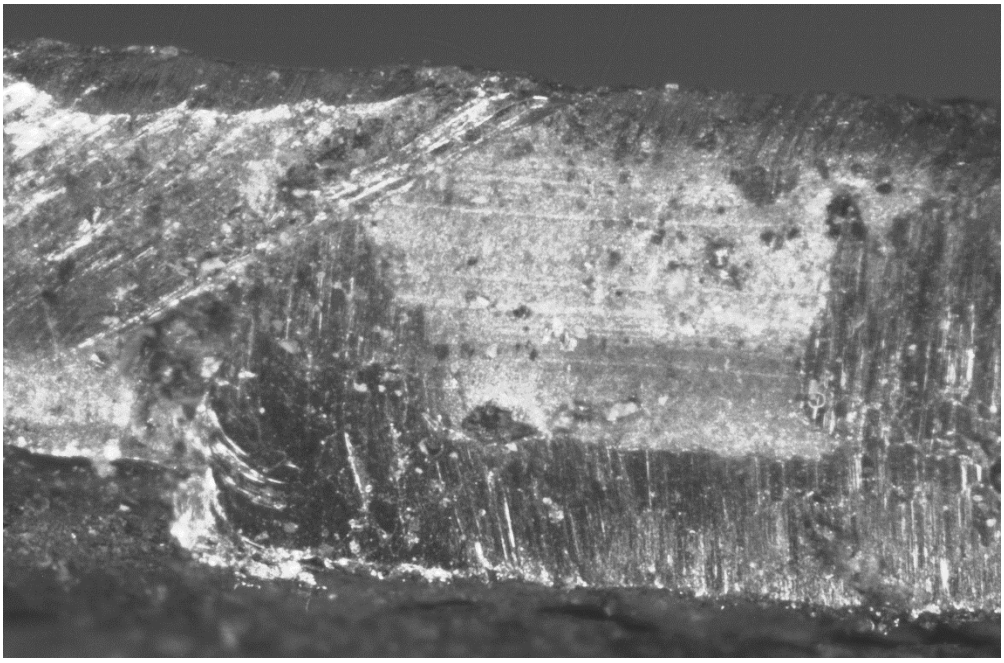

Figure 5 Beachmarks present on the fracture surface at the site of the original water leak, whose position was identified from the surface damage (seen here) inflicted by insertion of the screwdriver.

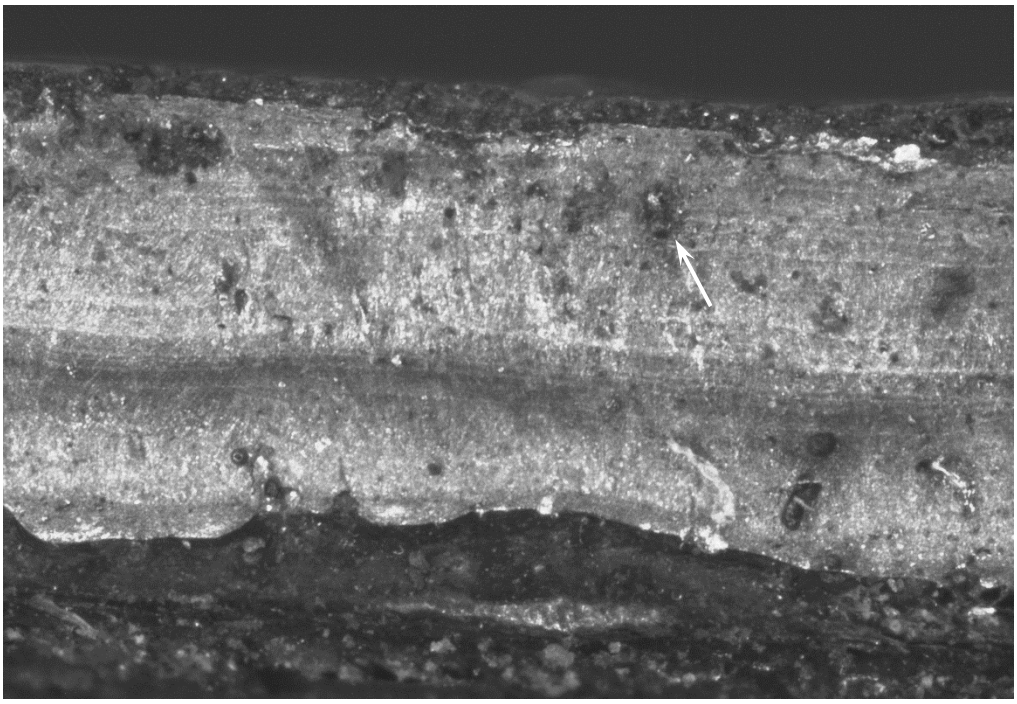

Figure 6 The beachmarks were present all along the fracture surface and therefore reflect influences other than mechanism changes.

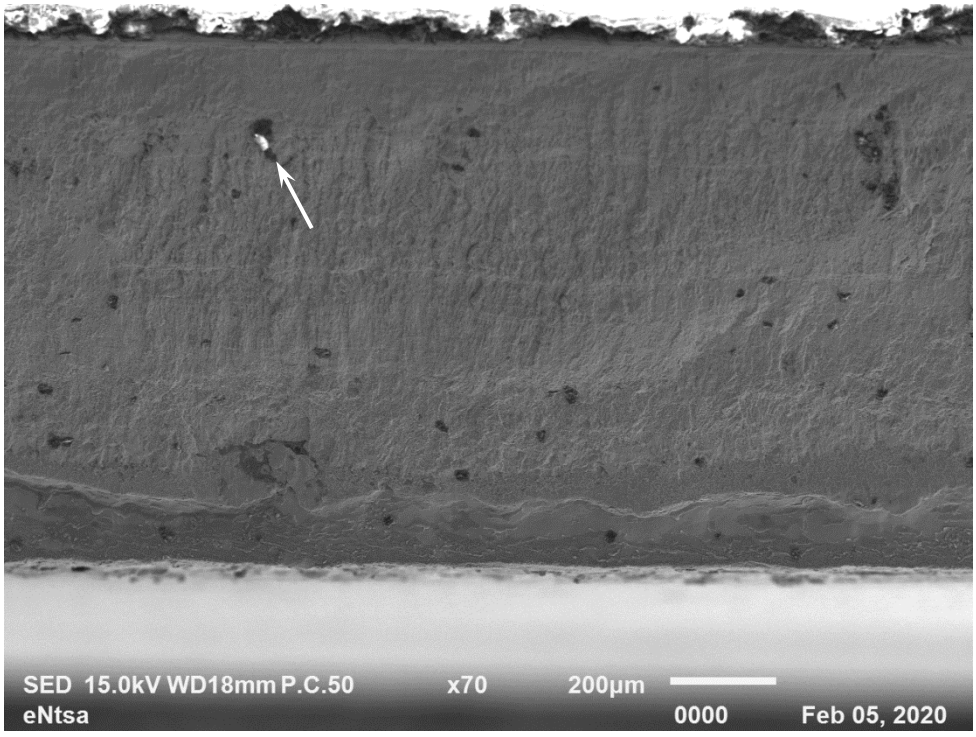

Figure 7 Low magnification SEM image of some of the region shown in Figure 5, with the weld root at the bottom of the image. The arrows in the two figures mark the same inclusion.

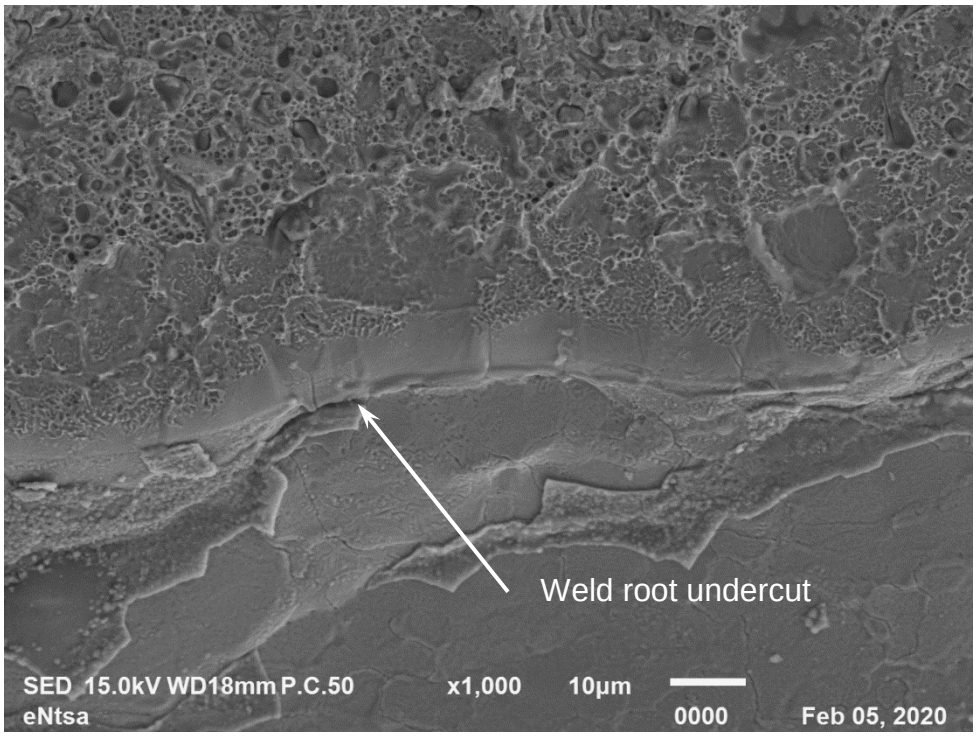

Figure 8 At high magnification the initial part of the fracture shows the partial penetration defect, a sharp weld root intrusion and the initial region of the solidification crack.

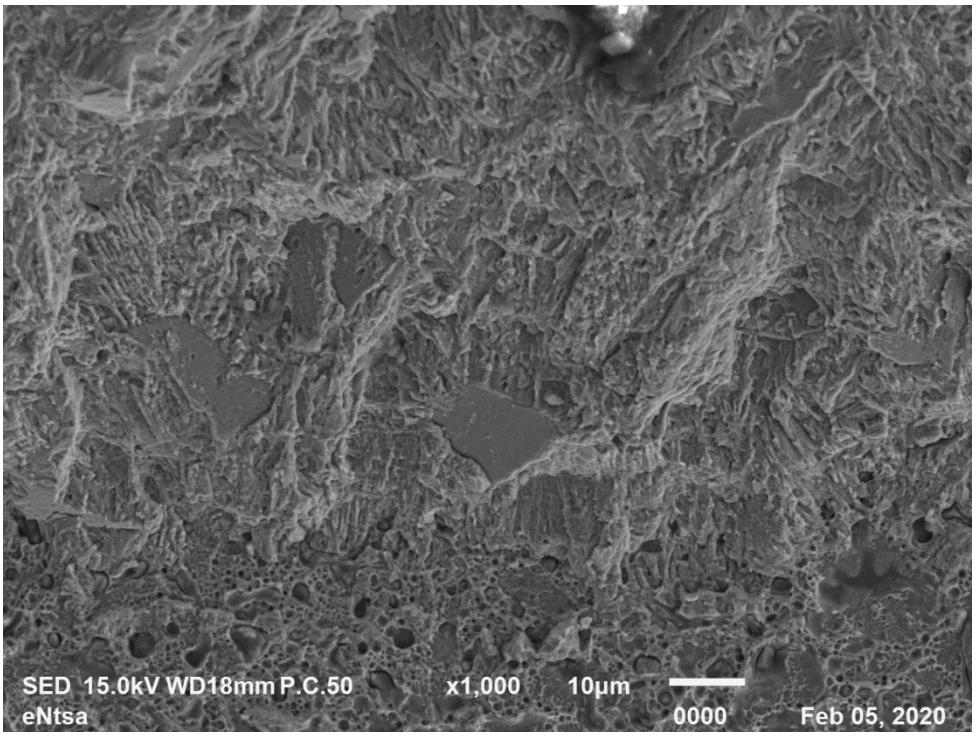

Figure 9 Transition from the initial solidification crack to a region that has an appearance typical of slow fatigue crack growth in 300 series austenitic alloys.

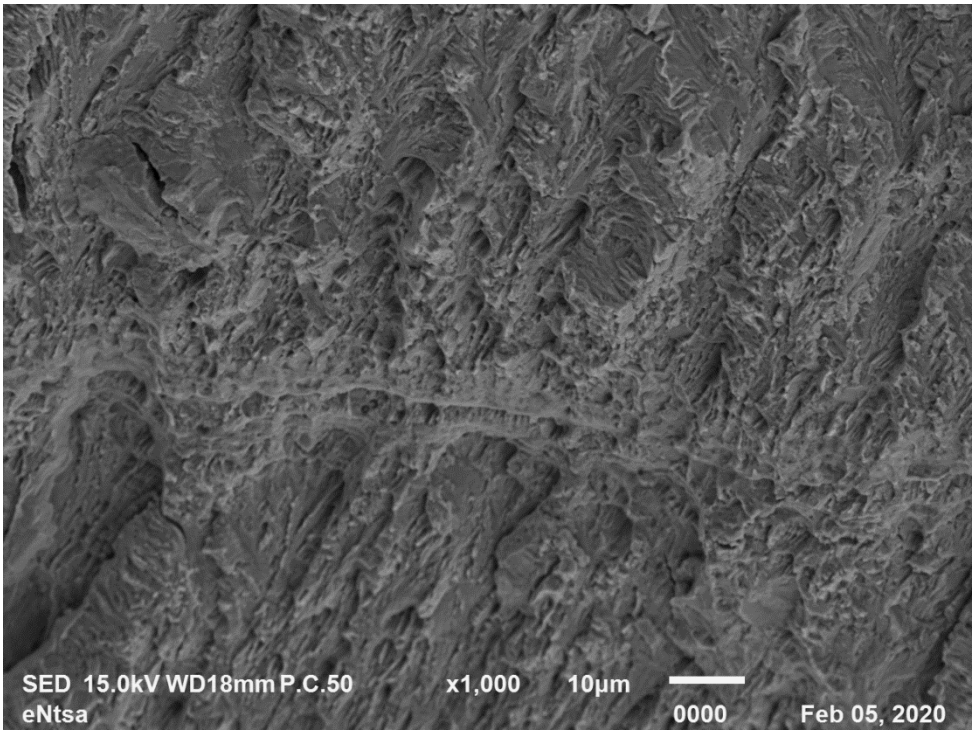

Figure 10 Brittle interdendritic fracture comprises the bulk of the fracture surface, reflecting microfissuring that opens up into a macro-crack under applied strain.

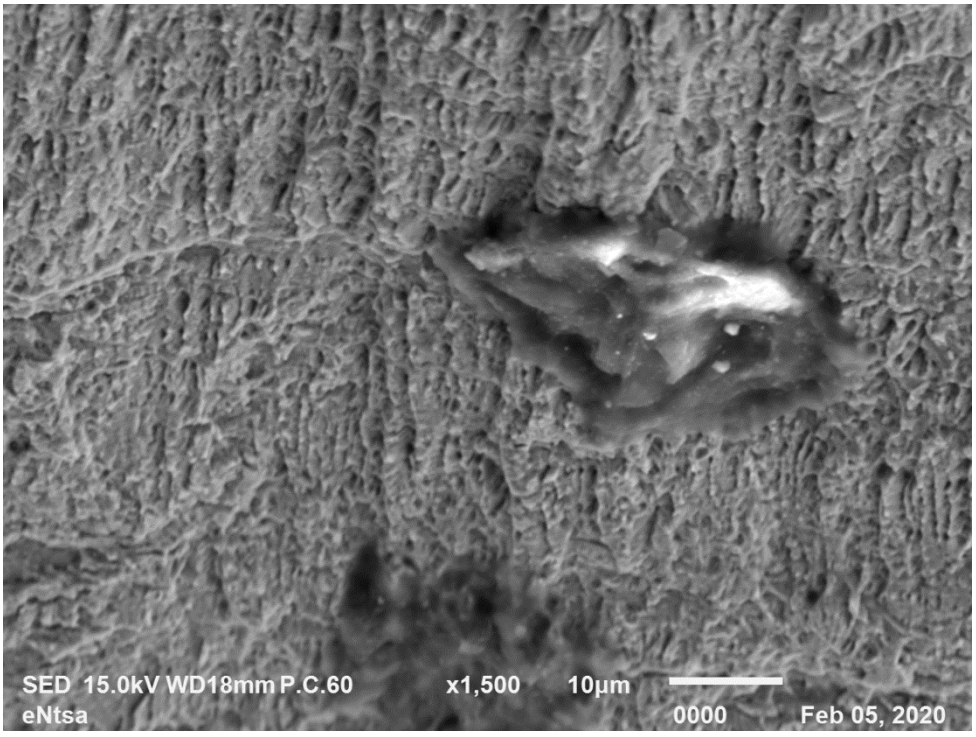

Figure 11 The mechanism of interdendritic fracture can be clearly seen in this image.

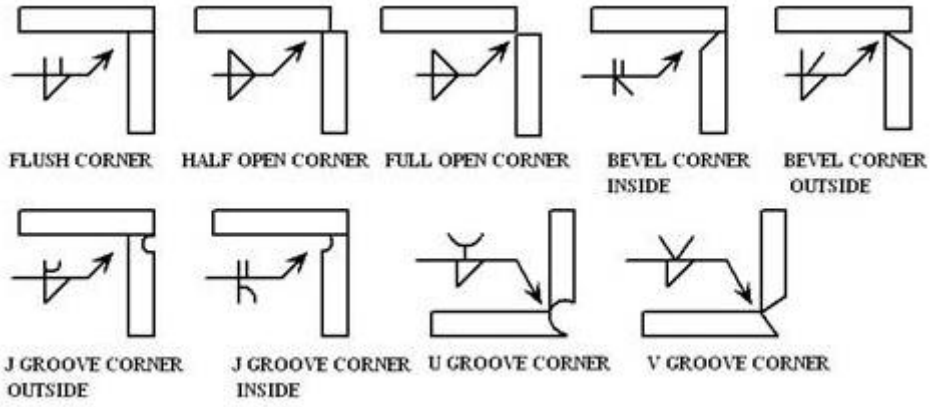

Figure 12 Types of corner joint edge preparation, illustrating the full-open or half-open corner joint that was used for the failed seam weld